UDC 655:535.361; 535.555
DOI: 10.20535/2077-7264.3(77).2022.274220

© Kh. Felde, PhD in physics and mathematics science, Associate professor, I. Soltys, PhD in physics and mathematics science, Associate professor, M. Havryliak, PhD in physics and mathematics science, Associate professor, A. Motrych, PhD in physics and mathematics science, Assistent, Yu. Ushenko, Doctor of physics and mathematics of science, Professor, V. Dvorzhak, PhD in physics and mathematics science, Associate professor, Chernivtsi National University, Chernivtsi, O. Liniuchev, PhD in technical science, Assistant, Igor Sikorskyi KPI, Kyiv, Ukraine

TECHNOLOGY OF PROTECTION AND CONTROL OF PRINTED PRODUCTS USING APPLICATION PROGRAMS OF DIGITAL INTROSCOPY

The article presents the basics of the method of correlation spatial-frequency filtering of maps of phase distributions of polyethylene films. Using the method of statistical analysis of the structure of spatial-frequency filtered polarization maps of polymer films, a set of methods and criteria for diagnosing changes in the birefringence of packaging materials has been substantiated and tested.

Keywords: programming method; graphic information processing; standardization; publishing; packaging materials; materials science.

Introduction

The fundamentals of the method of correlation filtering [1–3] of phase maps of images of polymer polyethylene films are presented. Comparative studies of the effectiveness of methods of direct polarization mapping of images [4–6] of polymer packaging films, as well as a spatial-frequency laser field transformed by filamentous optical inhomogeneous grids, have been carried out. Using a statistical analysis [7, 8] of the structure of spatially-frequency-filtered polarization maps of polymeric polyethylene films, a set of basic criteria for diagnosing changes in the anisotropy of packaging materials was studied.

This work is aimed at approbation of the principles of sequential spatial-frequency correlation differentiation of manifestations of linear and circular phase anisotropy of polycrystalline networks of polymer films for diagnostics of packing strength.

Method

On fig. 1 are shown the classical scheme of the polarimeter with spatial frequency filtering [9, 10].

ISSN 2077-7264. Технологія і техніка друкарства. 2022. № 3(77)

Irradiation of the investigation sample *6* was carried out by a parallel (L = 104 μm) beam of a He-Cd laser (λ = 0,6328 μm; W = 5 mW power). The polarizing illuminator consists of basic quarter-wave plates *3*, *5* and an optical polarizer *4*, which ensures the formation of a laser beam with an arbitrary azimuth $0° \le \alpha_0 \le 180°$ or ellipticity $0° \le \beta_0 \le 90°$ of polarization.

Polyethylene films were placed at the focal plane of a polarizing of the microlens *7* (FL f = 30 mm, magnification: 4X, DA N. A. = 0,1).

Low-frequency or high-frequency filters were located in the rear focal plane.

The polarizing microobjective *9* (focal length f = 30 mm, magnification 4X, digital aperture N. A. = 0,1) was located at the focal length from the frequency plane of the objective *7* and, therefore, carried out the inverse Fourier transform of the spatially-frequency filtered laser radiation field.

The coordinate distribution of the intensity of such a field was recorded in the plane of the photosensitive high resolution CCD camera *12* (the size of the photosensitive area of the N = m×n = 1280×920 pixels), which was also located at the focal distance from the microobjective *9* and provided a measurement range of the structural elements of the reconstructed image of polymer polyethylene films for geometric dimensions of 2–2000 μm.

The parameters of the Stokes vector of the spatial-frequency filtered image were determined for each individual pixel

$$S_1 = I_0 + I_{90};$$
$$S_2 = I_0 - I_{90};$$
$$S_3 = I_{45} - I_{135};$$
$$S_4 = I_{right} - I_{left}. \qquad (1)$$

here I_0; I_{90}; I_{45}; I_{135} — intensities of linearly (azimuths: 0°; 90°; 45°; 135°) and left — I_{left} and right — I_{right} circularly polarized laser beam transmitted by the system quarter-wave plate *10* and polarizer *11*.

Results

It were two types of optically thin (attenuation coefficient $\tau \approx 0{,}075 \div 0{,}083$) polyethylene films groups:

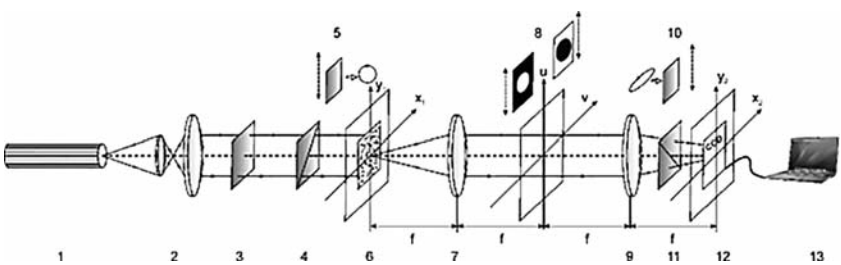

Fig. 1. Optical scheme of the polarimeter with spatial frequency filtering, where 1 — He-Ne laser; 2 — collimator; 3 — basic quarter-wave plate; 5, 10 — mechanically moving quarter-wave plates; 4, 11 — two polarizers; 6 — objects plane; 7, 9 — optical microobjectives; 8 — low-frequency and high-frequency filters (low-frequency and high-frequency); 12 — high resolution CCD camera; 13 — PC (special software)

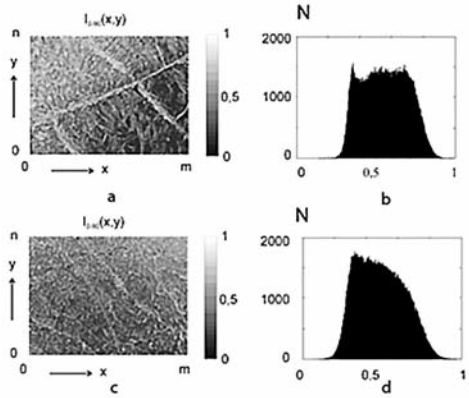

Fig. 2. Statistical (b, d) characteristics of the polarization image of polymer polyethylene films: group 1(a) and group 2(b)

— group 1 — stable (without deformation) (N = 21 — number of samples);

— group 2 — with mechanical deformftion (N = 19 — number of samples).

Fig. 2 shows images of the statistical structure of polyethylene polymer films obtained in a crossed polarizer and analyzer.

As can be seen from the fig. 2 that polarization-visualized images of the optical-inhomogeneous component of the samples and the geometric structure of their polycrystalline birefringence network consists of two main fragments — large-scale whiskers and small-scale deep crystals.

Comparative analysis of histograms (fig. 2, b, d) of intensity distributions did not reveal significant differences between this two groups of polymers.

The results of the investigation of the azimuth and ellipticity coordinate distributions of both types of polymer polyethylene films are shown in fig. 3, 4.

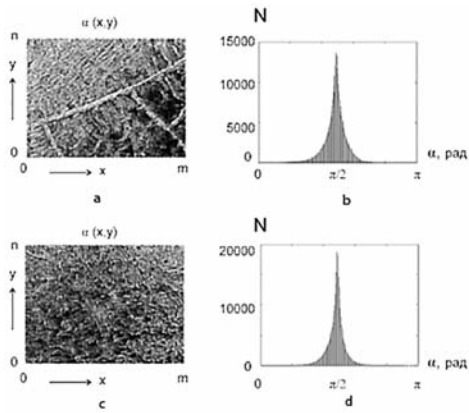

Fig. 3. Polarization maps (a, c) and their histograms (b, d) of polarization azimuths $\alpha(x, y)$ of polymer films (group 1 (a, b) and group 2 (c, d)

ISSN 2077-7264. Технологія і техніка друкарства. 2022. № 3(77)

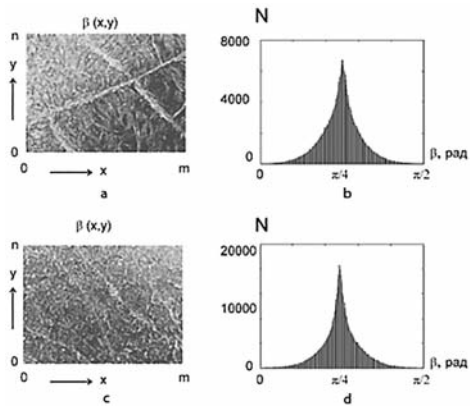

Fig. 4. Polarization maps (a, c) and their histograms (b, d) of polarization ellipticity β(x, y) of polymer films from group 1 (a, b) and group 2 (c, d)

Thus, the structure of polarization images of such phase-inhomogeneous layers is illustrated by a set of statistical moments (1–4 orders), that characterizing polarization maps α(x, y) and β(x, y) laser images as a combination of polyethylene polymer films from both groups (table 1).

Fig. 5, 6 shows the diagnostic capabilities of the Stokes polarimetry method using spatial frequency filtering for two groups of polymers.

Discussion

Data analysis of table 1 showed that the values of the set of statistical moments of all orders $M_{i=1;2;3;4} \approx \approx M^*_{i=1;2;3;4}$ within the standard deviation determined for the laser polarization maps images of polyethylene polymer films, taken from group 1 and group 2, 'overlap' and cannot be used as objective parameters of their differentiation. Thus, the problem of increasing the sensitivity of using method by means of spatial-frequency separation is relevant.

Table 1

Statistical moments of azimuth and ellipticity polarization maps of polyethylene polymer films

Parameters	α(x, y)		Parameters	β(x, y)	
$M_{i=1;2;3;4}$	Group 1 (number of samples — 21)	Group 2 (number of samples — 19)	$M^*_{i=1;2;3;4}$	Group 1 (number of samples — 21)	Group 2 (number of samples — 19)
M_1	1,62±0,28	1,64±0,31	M^*_1	0,28±0,039	0,33±0,044
M_2	0,085±0,014	0,071±0,011	M^*_2	0,12±0,018	0,095±0,013
M_3	0,28±0,041	0,33±0,049	M^*_3	0,11±0,015	0,14±0,019
M_4	2,12±0,36	2,77±0,43	M^*_4	1,78±0,27	1,99±0,38
$M_{i=1;2;3;4} \approx M^*_{i=1;2;3;4}$					

ISSN 2077-7264. Технологія і техніка друкарства. 2022. № 3(77)

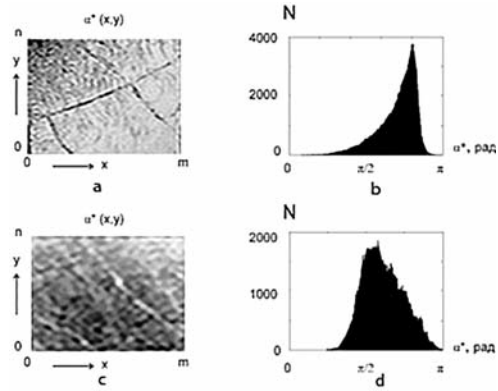

Fig. 5. Large-scale polymer polarization map (a, c), histogram (b, d), distributions of the polarization azimuth of polyethylene polymer films (group 1 (a, b) and group 2 (c, d)

A comparative analysis of the set of statistical data characterizing the polarization maps of the azimuth $\alpha^*(x, y)$ of a large-scale image (with predominantly linear birefringence) of crystals network revealed certain differences between them.

Another figure characterized the statistical analysis of the coordinate distributions of the azimuth maps that formed by circularly birefringent networks of 'small-scale' crystals — fig. 6.

Comparison of the data obtained revealed a significant expansion of the range of change in the distribution of random values $\alpha^{**}(x, y)$ of the histogram determined for the spatially-frequency filtered polarization map of a polycrystalline network with predominant circular birefringence.

Quantitative differences between the polarization maps of the azimuth of images of polycrystalline networks are shown in table 2.

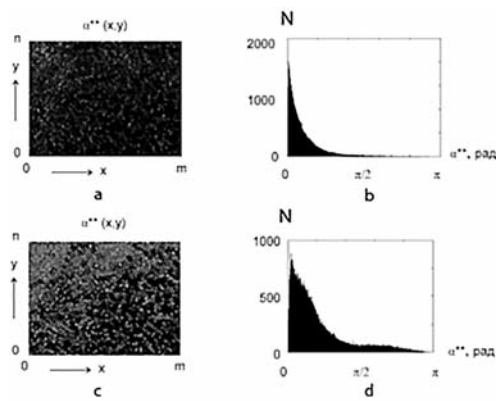

Fig. 6. Small-scale polymer map (a, c), histogram (b, d), of azimuth of polyethylene polymer films ((group 1 (a, b) and group 2 (c, d))

ISSN 2077-7264. Технологія і техніка друкарства. 2022. № 3(77)

Table 2

Statistical structure of polarization maps of azimuth of polycrystalline networks of polyethylene films from both groups

Parameters	LS $\alpha^*(x, y)$		SC $\alpha^{**}(x, y)$	
	Group 1 (number of samples — 21)	Group 2 (number of samples — 19)	Group 1 (number of samples — 21)	Group 2 (number of samples — 19)
M_1	1,07±0,17	1,12±0,19	0,27±0,037	0,35±0,046
M_2	0,14±0,021	0,19±0,025	0,082±0,012	0,19±0,031
M_3	1,73±0,24	0,16±0,027	0,11±0,017	1,03±0,15
M_4	0,89±0,011	0,12±0,017	1,54±0,22	0,63±0,077

Differntiation sensitive growth parameters of circular birefringence of polycrystalline networks of polyethylene films from group 2 (analysis from group 2):

— statistical moments of the 3rd and 4th orders, characterizing the coordinate distributions $\alpha^*(x, y)$ of the low-frequency component of the polarization azimuth map. Differences between their values ranging from 7 (M_3) to 10 (M_4) times;

— statistical moments of the 2nd–4th order of distributions, characterizing the coordinate distributions $\alpha^{**}(x, y)$ of the high-frequency component of the polarization azimuth map. Differences between their values ranging from 2 (M_2, M_3) to 10 (M_4) times.

Conclusions

1. The method of polarization mapping of optically inhomogeneous polycrystalline grids of polymeric polyethylene films with spatial-frequency filtering of the coordinate distributions of the laser beam polarization azimuth in the Fourier plane is described analytically.

2. Comparative studies of the efficiency of using direct mapping methods with spatial-frequency selection for differentiating the distributions of the azimuth and ellipticity of laser radiation converted by grids of polymer polyethylene films have been carried out.

3. A set of criteria for diagnosing and differentiating mechanical deformations of packaging polyethylene films was tested on the basis of statistical (statistical moments of the 1st–4th orders) analysis of spatially-frequency-filtered polarization images.

References

1. (2002). Handbook of Optical Coherence Tomography / edited by B. E. Bouma and G. J. Tearn // *Polarization-sensitive optical coherence tomography* / de Boer, J. F., Milner, T. E., Ducros, M. G., Srinivas, S. M., & Nelson, J. S. New York: Marcel Dekker Inc., 237–274.

2. Ghosh, S., Herink, G., Perri, A., Preda, F., Manzoni, C., Polli, D., & Cerullo, G. (2022, 4 March). Rapid and high-sensitivity measurements of broadband

ISSN 2077-7264. Технологія і техніка друкарства. 2022. № 3(77)

optical activity with interferometric Fourier-transform balanced detection. *Proc. SPIE 11986, Real-time Measurements, Rogue Phenomena, and Single-Shot Applications VII*, 1198606.

3. Sankaran, V., Everett, M. J., Maitland, D. J., & Walsh, J. T. (1999). Comparison of polarized-light propagation in biological tissue and phantoms. *Opt. Lett*, Vol. 24, 1044–1046.

4. Meng, X., Li, J., Zhang, Y., & Zhu, R. (2014, 18 November). System calibration of Stokes imaging polarimeter using Fourier series analysis. *Proc. SPIE 9299, International Symposium on Optoelectronic Technology and Application 2014: Optical Remote Sensing Technology and Applications*, 92991E.

5. Berezhna, S., Berezhnyy, I., Takashi, M., & Voloshin, A. (2001). Full-field automated photoelasticity by Fourier polarimetry with three wavelengths. *Appl. Opt.*, 40, 52–61.

6. Mujica, R., Augustine, A., Pauly, M., Houerou, V. L., Decher, G., Battie, Y., & Felix, O. (2022). Macroscopic mapping of the linear in-plane anisotropy of nanocellulosic thin films by Mueller matrix polarimetry. *Composites Science and Technology*, Vol. 233, 109889.

7. Hinrichs, K., Blevins, B., Furchner, A., Yadavalli, N. S., & Minko, S. (2022). Infrared polarimetry: Anisotropy of polymer nanofibers. *Micro and Nano Engineering*, Vol. 14, 100116.

8. Losmanschii, C., Achimova, E., Abashkin, V., Botnari, V., & Meshalkin, A. (2022). Photoinduced Anisotropy in Azopolymer Studied by Spectroscopic and Polarimetric Parameters. In: Tiginyanu, I., Sontea, V., Railean, S. (eds) 5th International Conference on Nanotechnologies and Biomedical Engineering. ICNBME 2021. *IFMBE Proceedings*, vol. 87. Springer, Cham.

9. Sumihara, K. A., Okubo, S., Oguchi, K., Inaba, H., & Watanabe, S. (2019). Development of Polarization-Sensitive Dual-Comb Spectroscopy for Anisotropic Materials. *Conference on Lasers and Electro-Optics Europe & European Quantum Electronics Conference (CLEO/Europe-EQEC)*, 1–1.

10. Ushenko, A. G., Misevich, I. Z., Istratiy, V., Bachyns'ka, I., Peresunko, A. P., Numan, O. K., & Moiysuk, T. G. (2010). Evolution of statistic moments of 2D-distributions of biological liquid crystal netmueller matrix elements in the process of their birefringent structure changes. *Advances in Optical Technologies*. ID 423145.

У статті наведено основи методу кореляційної просторово-частотної фільтрації карток фазових розподілів поліетиленових плівок. Використовуючи метод статистичного аналізу структури просторово-частотних фільтрованих поляризаційних карт полімерних плівок, обґрунтовано та апробовано комплекс методів та критеріїв діагностики зміни двопроменеломлення пакувальних матеріалів.

Ключові слова: прикладне програмування; обробка графічної інформації; стандартизація; поліграфія; пакувальні матеріали; матеріалознавство.

Надійшла до редакції 04.10.22